Available online at www.sciencedirect.com
ScienceDirect
Journal of Photochemistry and Photobiology A: Chemistry 193 (2008) 50–55
Journal of Photochemistry and Photobiology A:Chemistry
www.elsevier.com/locate/jphotochem

The ferrioxalate and iodide–iodate actinometers in the UV region

Sara Goldstein, Joseph Rabani *

Department of Physical Chemistry, The Hebrew University of Jerusalem, Jerusalem 91904, Israel

Received 26 February 2007; received in revised form 6 June 2007; accepted 8 June 2007
Available online 14 June 2007

Abstract

The ferrioxalate and iodide–iodate actinometers have been re-studied in view of apparent inconsistencies and disagreements of results obtained using different methods and laboratories. The quantum yields have been determined with the aid of highly accurate and sensitive calibrated photodiodes in the range 205–365 nm. In the case of ferrioxalate, a pronounced change between 240 and 270 nm was observed with a plateau below 240 nm, $\Phi(Fe^{II}) = 1.48 \pm 0.02$, and above 270 nm, $\Phi(Fe^{II}) = 1.25 \pm 0.02$. The latter value agrees with other literature reports and is attributed to the known ligand to metal charge transfer band around 300 nm. A shoulder at 215–230 nm is apparently associated with the higher quantum yield below 240 nm. The quantum yield of I_3^- in the iodide–iodate system is essentially constant between 205 and 245 nm, $\Phi(I_3^-) = 0.92 \pm 0.02$. The results agree with part of the literature values and provide reliable $\Phi(I_3^-)$ for the range 205–290 nm for the purpose of actinometry. The steep change above 245 nm introduces a high uncertainty unless well-defined monochromatic light is used. The integrated results of both actinometers are consistent, and apparent discrepancies in literature are resolved.

Keywords: Ferrioxalate; Iodide–iodate; Actinometer; Quantum yield

1. Introduction

The ferrioxalate actinometer, first introduced by Hatchard and Parker [1,2], is probably the most commonly used. The quantum yield of Fe^{II}, which is partially complexed, $\Phi(Fe^{II})$, has been measured between 254 and 587 nm by comparison with a thermopile, increasing with decreasing wavelength up to 1.24 ± 0.04 below 365 nm [1,2]. These results have been confirmed using either calibrated thermopile [3] or electrical radiometer [4] in the range 365–458 nm. The quantum yield at wavelengths shorter than 254 nm was studied by Fernandez et al. [5], who reported a relatively high quantum yield of 1.35 at 248 nm, although unexpected much lower values below 240 nm.

The iodide–iodate actinometer has been introduced by Rahn [6,7] who measured the quantum yield of the product I_3^- spectrophotometrically. This actinometer is optically opaque to light below 290 nm and is optically transparent to wavelengths greater than 330 nm. The actinometer solution absorbs practically all of the light below 290 nm in 1 cm path but in contrast to the ferrioxalate little if any of the ambient light normally present in the laboratory. Recently, Rahn et al. [8], reported inconsistencies between I_3^- yields in the iodide–iodate system, based on radiometry and ferrioxalate actinometry. The latter showed 20% reduction in the yield between 240 and 280 nm compared with the radiometry, taking $\Phi(Fe^{II}) = 1.25$. They concluded that the quantum yield of the ferrioxalate at this region of the spectrum needs reexamination. A recent publication [9] acknowledged that different recommendations in the literature concerning the adequate use of the ferrioxalate actinometer resulted with different observations. The IUPAC subcommittee on Photochemistry (2004) recommended that publications contain an unequivocal indication as to which experimental conditions have been applied [9].

In view of the above discrepancy and in light of different results obtained by different methods and laboratories [6,7], we have reexamined the quantum yields of both actinometers in the range 205–320 nm, with the aid of a highly accurate and sensitive calibrated silicon photo-diode.

2. Experimental

2.1. Materials and analysis procedure

The ferrioxalate actinometer [1,2,10] was prepared by mixing equal volumes of 0.02 M ammonium ferric sulfate dodecahy-

* Corresponding author. Tel.: +972 2 6585292; fax: +972 2 6586925.
E-mail address: rabani@vms.huji.ac.il (J. Rabani).

1010-6030/$ – see front matter © 2007 Elsevier B.V. All rights reserved.
doi:10.1016/j.jphotochem.2007.06.006

drate (Fluka, Ultra) with 0.06 M potassium oxalate-1-hydrate (Riedel-de-Haen, Analytical) both in 0.1N H_2SO_4 (Aldrich 95–98%) in the dark or red light. After illumination the product Fe^{2+} was analyzed by adding 0.5 mL of 0.1% (w/v) 1,10-phenanthroline monohydrate (Fluka, puriss) in 1.8 M anhydrous sodium acetate (Merck, Analytical) to 3 mL of the actinometer. The absorbance of $Fe(1,10\text{-phen})_3^{2+}$ was measured after 30 min in the dark using $\varepsilon_{510} = 11100\,M^{-1}\,cm^{-1}$ for the calculation of the concentration. The optical absorption after 30 min was stable in the dark, although it continued to increase upon exposure to room light.

The iodide–iodate actinometer was prepared daily and contained 0.6 M potassium iodide and 0.1 M potassium iodate in 0.01 M $Na_2B_4O_7{\cdot}12\ H_2O$, "99.5–105%" at pH 9.25 (all three products of Sigma–Aldrich, reagent grade). The actinometer was used in room light. Determination of the photo-product I_3^- was carried out spectrophotometrically using $\varepsilon_{352} = 27{,}600\,M^{-1}\,cm^{-1}$ [8]. All solutions were prepared with deionized water, which was purified using a Milli-Q water purification system.

2.2. Photolysis

Two light sources were used: (i) monochromatic low-pressure Mercury lamp (Heraeus NNI 120/44U, with the 185 nm line filtered out). The monochromatic light passed through a 10 cm long tube located between the lamp and the sample. A narrowband (10 nm) interference filter for 253.7 nm (12 nm band, 16% peak transmittance) was always used to eliminate the light from other wavelengths. The incident light intensity was controlled by changing the distance between the lamp and the sample. (ii) A Xenon lamp (Osram 150 W ozone free) coupled with a monochromator (SX-17MV setup from Applied Photophysics). The slits of the monochromator were adjusted to provide a bandwidth of 4.7 nm. In addition, appropriate narrowband interference filters (10–12 nm, 14–22% peak transmittance) were usually used below 300 nm to assure complete elimination of scattered light. Direct measurements of scattered light by comparison between the light-signal at a given wavelength to that at 170 nm (where the light intensity is zero) showed only 0.5% scattered light at 280 nm increasing to about 4% at 225 nm. Nevertheless, some iodide–iodate tests were carried out at 225–250 nm without interference filters, and were corrected for scattered light. Irradiations were carried out in cylindrical cells (2 cm i.d., 1- or 2-cm length) made entirely from Suprasil quartz under magnetic stirring at room temperature ($24 \pm 1\,^{\circ}C$). The light entered through a flat optical window. It has been reported that the quantum yield of ferrioxalate does not depend on the temperature [2,11], whereas that of iodide–iodate increases by 2% per each degree at 254 nm [7]. The 1-cm long cell was used with the Xenon light source and the 2-cm long cell was used with the Mercury lamp. The cells had short side arms with glass taper joints, through which actinometer solutions were introduced. A small stirrer was placed in the solutions outside the light path. The volumes of the illuminated solutions (including a small amount in the side arms, corrected for the stirrer) were measured as 3.07 and 6.67 mL, respectively. This was calculated from the difference in the weight of the cell, stirrer and stopper with and without water using $d = 0.997\,g/cm^3$. The incident light intensity was measured with a sensitive calibrated Si photo-sensor (Hamamatsu S2281, recalibrated by the Physikalisch-Technische-Bundesanstalt in Berlin) coupled with a Keithley 617 programmable electrometer. Another radiometer (PD300-UV coupled with LaserStar display by Ophir Optronics Inc.), which was calibrated against a NIST standard, was used for confirmation. At 253.7 nm the two radiometers differed by 2.4%. Nevertheless, the quantum yields were based on the Hamamatsu S2281 photo-sensor because its precision was better than 1%, whereas that of Ophir is 6% below 250 nm and 3% at higher wavelengths. The light passed through a small aperture of 0.794 cm (low-pressure lamp, iodide–iodate tests) or 0.635 cm diameter (all tests with the Xenon lamp) to ensure that the beam incident is smaller than the area of the radiometer ($d = 1.13$ cm) and the irradiated cell ($d = 2$ cm). The absorbed radiant power (W) was multiplied by $8.360 \times 10^{-6}\,\lambda/V$ (the wavelength λ expressed in nm, the volume of the solution V in mL) to obtain einstein $L^{-1}\,s^{-1}$. The radiant power measured by the radiometer was corrected by 4%, which accounts for the reflection of the incident light from the surface of the quartz cell (calculated as $R = (n_1 - n_2)^2/(n_1 + n_2)^2$, where R is the reflection coefficient and $n_1 = 1.516$ and $n_2 = 1.000$ are the respective refractive indices of quartz and air). No aperture was used when direct comparison between the two actinometers was carried out at 253.7 nm using the low-pressure lamp without employing the radiometer. In this case no correction for the loss of the incident light was made.

3. Results

3.1. Photolysis at 253.7 nm using the low-pressure Mercury lamp

The iodide–iodate and the ferrioxalate actinometer solutions were irradiated with an interference filter attached to the illumination cell. At a given light intensity, the product concentration increased linearly with exposure time as demonstrated in Fig. 1 for the iodide–iodate system. Quantum yields were derived by dividing the slopes of the lines, such as in Fig. 1, by the respective flux.

The results for I_3^- are summarized in Table 1, yielding an average quantum yield of 0.72 ± 0.03.

In a separate set of measurements the rate of Fe^{2+} formation in the ferrioxalate system was directly compared to that of I_3^-

Table 1
$\Phi(I_3^-)$ at 253.7 nm

Run no.	Rate of I_3^- formation ($M\,s^{-1}$)	Rate of UV absorption (einstein $L^{-1}\,s^{-1}$)	$\Phi(I_3^-)$
1	7.70×10^{-9}	1.06×10^{-8}	0.76
2	8.71×10^{-9}	1.18×10^{-8}	0.77
3	2.73×10^{-9}	3.98×10^{-8}	0.72
Average			0.75 ± 0.03[a]

[a] Standard deviation.

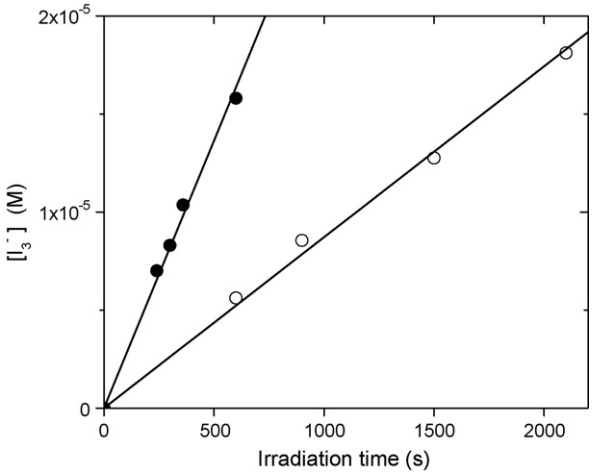

Fig. 1. The growth of I_3^- in the iodide–iodate system as a function of irradiation time at (◯) 1.18×10^{-8} and (●) 3.98×10^{-8} einstein L^{-1} s^{-1}. Irradiation was carried out with the low-pressure lamp and a 253.7 nm interference filter. An aperture of 0.794 cm diameter was placed in front of the illumination cell in order to assure that the same beam is absorbed by the radiometer and by the actinometer, respectively.

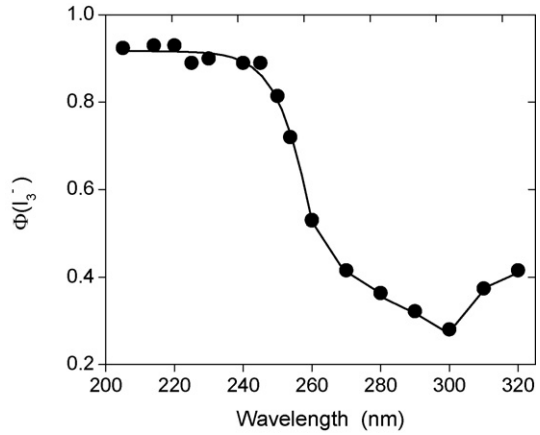

Fig. 2. Quantum yields of I_3^- in the iodide–iodate system as a function of wavelength. Each point represents an average of at least three results taken within the linear build-up region of I_3^-. Below 290 nm there is essentially total absorption by the solution and the light absorbed above 290 nm was calculated using Beer's law. The optical absorption measured in 1 cm cuvette was 2.00 at 290 nm, 0.620 at 300 nm, 0.187 at 310 nm and 0.200 at 320 nm (the latter measured in a 4 cm cuvette).

in the iodide–iodate at the same fluence rate. The results are summarized in Table 2, yielding $\Phi(Fe^{II})/\Phi(I_3^-) = 1.98 \pm 0.06$, corresponding to $\Phi(Fe^{II}) = 1.43$.

3.2. Photolysis at 205–365 nm using the Xenon lamp

The dependency of the product quantum yields on excitation wavelength in the iodide–iodate and ferrioxalate systems is shown in Figs. 2 and 3, respectively. A summary of the present and literature results is presented in Tables 3 and 4 for iodide–iodate and ferrioxalate, respectively. The quantum yields of I_3^- and Fe^{II} were measured independently. At 253.7 nm the respective values are 0.72 ± 0.02 and 1.40 ± 0.03, in excellent agreement with the results of the low-pressure Mercury lamp. Hence, the results of both lamps at 253.7 nm yields $F(I_3^-) = 0.72 \pm 0.02$ and $F(Fe^{2+}) = 1.41 \pm 0.04$.

Fig. 2 shows a plateau in the range 205–240 nm, corresponding to $\Phi(I_3^-) = 0.92 \pm 0.02$. Fig. 3 shows a plateau at 205–250 nm with $\Phi(Fe^{II}) = 1.48 \pm 0.02$ and at 270–340 with $\Phi(Fe^{II}) = 1.25 \pm 0.02$. The error limits represent the standard deviation. The sigmoidal curves were chosen for convenience.

Table 2
Comparison of the rates of Fe^{II} and I_3^- build-up at 253.7 nm

Run no.	Rate of I_3^- formation ($M\,s^{-1}$)	Rate of Fe^{II} formation ($M\,s^{-1}$)	Ratio[a]
1	1.30×10^{-7}	2.51×10^{-7}	1.93
2	1.19×10^{-7}	2.43×10^{-7}	2.04
3	2.76×10^{-7}	1.40×10^{-6}	1.97
Average			1.98 ± 0.06[b]

[a] Ratio between the rate of Fe^{II} and I_3^- formation.
[b] Standard deviation.

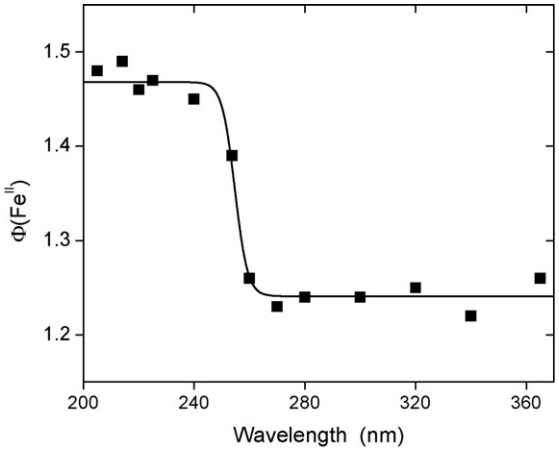

Fig. 3. Quantum yields of Fe^{II} in the ferrioxalate system as a function of wavelength. Each point represents an average of at least three results taken within the linear build-up region of Fe^{II}. The solutions contained 10 mM ferrioxalate in 0.1N H_2SO_4. There was essentially total absorption of the light in the entire wavelength range. Interference filters tightly attached to the illumination cell were used below 300 nm.

4. Discussion

The apparent discrepancy between $\Phi(I_3^-)$ based on radiometry and ferrioxalate actinometry below 254 nm [8] was caused because of ignoring the sharp increase of $\Phi(Fe^{II})$ from 1.24 at 270 nm to 1.45 at 240 nm (Fig. 3, Table 4). Above 260 nm the quantum yields in the ferrioxalate actinometer agree with earlier measurements at the respective wavelengths [2–4,11], although a plateau is observed above 270 nm. Fernandez et al. [5], determined $\Phi(Fe^{II}) = 1.35$ at 248 nm assuming that at 254 nm the value is 1.25. Taking the latter as 1.41, their value is revised to 1.52. At $\lambda < 248$ nm they observed a decrease in $\Phi(Fe^{II})$ compared to the plateau in Fig. 2 of the present work. The question of possible contribution of scattered light, however, has not been addressed in this work [5].

Table 3
$\Phi(I_3^-)$ at various wavelengths

λ (nm)	This work radiometry	BPI[a] or UAB[b] radiometry [8][c]	NIST radiometry [8]	Based on $\Phi(Fe^{II}) = 1.25$ [8]	Column 5 corrected for the revised $\Phi(Fe^{II})$ from Table 4
205	0.93 ± 0.04[d]				
214	0.94 ± 0.02[d]	0.84 (BPI)		0.78	0.93
220	0.94 ± 0.06[d]	0.82 (BPI)		0.83	0.98
225	0.89 ± 0.02[e]				
228		0.80 (BPI)		0.74	0.87
230	0.89 ± 0.02[e]	0.90 (UAB1) 0.67 (UAB2)			
234			0.82		
		0.95 (BPI)			
240	0.88 ± 0.03[e]	0.84 (UAB1) 0.83 (UAB2)		0.76	0.88
245	0.89 ± 0.02[e]	0.74 (UAB2)			
250	0.82 ± 0.02[e]	0.79 (UAB1) 0.79 (UAB2)			
253.7	0.71 ± 0.02[d] 0.74 ± 0.02[e]				
253.7	0.72 ± 0.03[f]	0.76 (BPI) 0.65 (BPI)	0.73	0.60	0.68
260	0.53 ± 0.02[d]	0.65 (UAB1) 0.65 (UAB2)		0.52	0.54
264			0.60		
	0.40 ± 0.02[d]	0.51 (BPI)			
270	0.43 ± 0.02[e]	0.43 (UAB1) 0.43 (UAB2)		0.44	0.44
274			0.44		
	0.37 ± 0.01[d]	0.37 (BPI)			
280	0.37 ± 0.01[e]	0.28 (UAB1) 0.25 (UAB2)			
284			0.30		0.30
290	0.32 ± 0.01[e]	0.25 (UAB1) 0.13 (UAB2)			
300	0.28 ± 0.01[e]	0.28 (UAB1) 0.13 (UAB2)			
310	0.38 ± 0.01[e]	0.38 (UAB1) 0.20 (UAB2)			
320	0.43 ± 0.02[e]	0.39 (UAB1) 0.44 (UAB2)			

[a] BPI stands for Bolton Photosciences Inc.
[b] UAB stands for University of Alabama at Birmingham.
[c] Normalized to 0.73 at 253.7 nm.
[d] Monochromator with interference filter.
[e] Monochromator without interference filter.
[f] Mercury lamp with interference filter.

Very good agreement is observed comparing our results of $\Phi(I_3^-)$ based on radiometry (Fig. 2 and Table 3, column 2) with the earlier values, which were based on the ferrioxalate actinometry [8] and recalculated using our revised $\Phi(Fe^{II})$ from Fig. 3 (see Table 3, columns 2 and 6). Discrepancies, however, exist between radiometry based $\Phi(I_3^-)$ values measured earlier in different laboratories [8]. The different values are presented in Table 3, columns 3 and 4. With the exception of the results at 245 and 260 nm, $\Phi(I_3^-)$ values reported here (Table 3, column 2) agree reasonably well with at least one of the parallel measurements reported earlier [8] (compare Table 3, columns 2, 3, and 4). Note that unlike the ferrioxalate, which essentially absorbs all the light in the entire range used here, the iodide/iodate actinometer absorbs more than 99.9% only below 285 nm. The absorption amounts to 99.0, 76.0, 35.0 and 10.9% at 290, 300, 310 and 320 nm, respectively. Nevertheless, the

Table 4
$\Phi(Fe^{II})$ in the ferrioxalate system at various wavelengths

λ (nm)	Incident light intensity (einstein s^{-1})	$\Phi(Fe^{II})$ This work	Literature results
205[a]	5.29×10^{-13}	1.49 ± 0.02	
214[a]	6.77×10^{-13}	1.50 ± 0.06	
220[a]	6.65×10^{-13}	1.47 ± 0.02	
222			0.5 [5]
225[a]	6.25×10^{-13}	1.46 ± 0.06	
230			0.67 [5]
240[a]	2.48×10^{-12}	1.45 ± 0.03	
248			1.35[5]
253.7[a]	5.62×10^{-12}	1.40 ± 0.03	1.25 [2]
260[a]	7.84×10^{-12}	1.26 ± 0.02	
270[a]	8.93×10^{-12}	1.24 ± 0.01	
280[a]	1.99×10^{-11}	1.25 ± 0.03	
300[a]	1.56×10^{-11}	1.25 ± 0.01	1.24[2]
313			1.24 ± 0.02 [2]
320[b]	1.33×10^{-10}	1.27 ± 0.02	
334			1.23 [2]
340[b]	1.39×10^{-10}	1.23 ± 0.02	
363.8			1.283 ± 0.023 [4]
365[b]	1.55×10^{-10}	1.27 ± 0.02	1.21 [2]; 1.26 ± 0.03 [3]

[a] Monochromator with interference filter.
[b] Monochromator without interference filter.

absorbance at these wavelengths could be accurately measured (using 4 cm cuvette at 320 nm, $D_{320} = 0.200$). Moreover, the light geometry in the cuvette was such that there were no internal reflections so that the correction for the absorption according to Beer's law was simple. The increase of $\Phi(I_3^-)$ above 300 nm is unexpected, although it was observed also earlier [8]. While the measured I_3^- at all wavelengths is accurate, small traces of unknown impurities may introduce uncertainty to $\Phi(I_3^-)$ above 300 nm due to the low absorption of the actinometer solution.

The sharp change of $\Phi(Fe^{II})$ between 250 and 270 nm can be attributed to different absorption bands. The spectrum of ferrioxalate is shown in Fig. 4. Addition of excess of 15% oxalate ions had no effect on the spectrum. Ferrous oxalate absorption is lower than that of ferrioxalate in the studied range. Under the conditions of this work, the product accumulated to less than

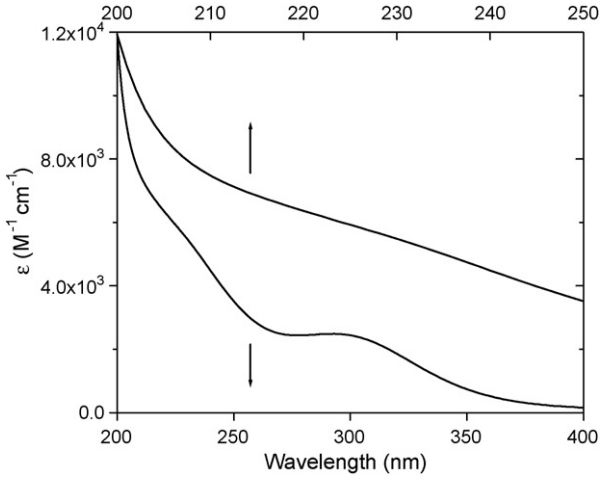

Fig. 4. The spectrum of ferrioxalate in 0.1N H_2SO_4. The upper curve represents the same spectrum at 200–250 nm, expanded wavelength scale.

0.4% of the ferrioxalate and its optical absorption was ignored.

This, and the high stability constant of the ferrioxalate rule out the possibility that free Fe^{3+} or its sulfate complex have a measurable contribution to the optical absorption. The spectrum shows the known ligand to metal charge transfer (LMCT) band with a peak near 300 nm, to which $\Phi(Fe^{II}) = 1.24$ is related. The shoulder at 215–230 nm represents a higher energy transition apparently associated with the higher quantum yield presented in Fig. 3. The increased quantum yield may be attributed to charge transfer to the water (CCTS). While excitation at the LMCT band produces Fe^{2+}, $C_2O_4^{\bullet -}$ and oxalate (reaction (1)), the CTTS results in the formation of e_{aq}^- and $Fe(C_2O_4)_3^{2-}$, where the radical is on the oxalate ion (reaction (2)).

$$Fe(C_2O_4)_3^{3-} \xrightarrow{h\nu} Fe^{2+} + C_2O_4^{\bullet -} + 2C_2O_4^{2-} \quad (1)$$

$$Fe(C_2O_4)_3^{3-} \xrightarrow{h\nu} Fe(C_2O_4)_3^{2-} + e_{aq}^- \quad (2)$$

The quantum yield $\Phi(Fe^{II}) = 1.24$ is determined by the competition between dissociation of the excited state and returning to the electronic ground state and by the competition between the reactive products of reaction (1) in the photochemical cage and their diffusion to the bulk of the solution. $C_2O_4^{\bullet -}$ (or $HC_2O_4^{\bullet}$) decomposes in the bulk to CO_2 and $CO_2^{\bullet -}$ (or $HCO_2^{\bullet}$) according to reaction (3) with subsequent reduction of ferrioxalate by the latter radical (reaction (4)).

$$C_2O_4^{\bullet -} \rightarrow CO_2 + CO_2^{\bullet -} \qquad k_3 = 2 \times 10^6\ s^{-1}\ [12] \quad (3)$$

$$CO_2^{\bullet -} + Fe(C_2O_4)_3^{3-} \rightarrow CO_2 + Fe^{2+} + 3C_2O_4^{2-}$$
$$k_4 = 10^9\text{–}10^{10}\ M^{-1}\ s^{-1}\ [13] \quad (4)$$

Excitation at the presumably CTTS band produces e_{aq}^- and $Fe(C_2O_4)_3^{2-}$ pair (reaction (2)), which may back react or diffuse out of the cage. The competition between these two processes determines $\Phi(Fe^{II}) = 1.48$. Alternatively, $Fe(C_2O_4)_3^{2-}$ may decompose in the cage according to reaction (5). In such a case, the competition between cage escape and cage reaction is more complicated as e_{aq}^- may react with Fe^{3+} or $C_2O_4^{\bullet -}$.

$$Fe(C_2O_4)_3^{2-} \rightarrow Fe^{3+} + 2C_2O_4^{2-} + C_2O_4^{\bullet -} \quad (5)$$

In 0.1N H_2SO_4, e_{aq}^- is converted to $H^{\bullet}$ in the bulk and to small extent in the cage. This does not affect the above discussion, although reduction by $H^{\bullet}$is usually slower. In any case a small fraction of the reducing radicals react with O_2 producing $HO_2^{\bullet}$, which most probably reduces ferrioxalate to Fe^{II} [14].

5. Conclusions

$\Phi(Fe^{II}) = 1.48 \pm 0.02$ is recommended for the ferrioxalate actinometry in the range 205–240 nm and $\Phi(Fe^{II}) = 1.25 \pm 0.02$ at 270–340 nm. $\Phi(Fe^{II})$ changes relatively very steeply in the range 254–260 nm and apparent values of $\Phi(Fe^{II})$ may be obtained at different wavelength resolutions. Hence, in this range very well-defined monochromatic light should be used. The

iodide–iodate system is particularly useful below 245 nm, where $\Phi(I_3^-) = 0.92 \pm 0.02$.

Acknowledgment

This research was partially supported by grant from the Israel Science Foundation of the Israel Academy of Sciences.

References

[1] C.A. Parker, A new sensitive chemical actinometer. I. Some trials with potassium ferrioxalate, Proc. R. Soc. A 220 (1953) 104.
[2] C.G. Hatchard, C.A. Parker, A new sensitive chemical actinometer. II. Potasium ferrioxalate as a standard chemical actinometer, Proc. R. Soc. A 235 (1956) 518–536.
[3] J. Lee, H.H. Seliger, Quantum yield of ferrioxalate actinometer, J. Chem. Phys. 40 (1964) 519–523.
[4] J.N. Demas, W.D. Bowman, E.F. Zalewskl, R.A. Velapoldl, Determination of the quantum yield of the ferrioxalate actinometer with electrically calibrated radiometers, J. Phys. Chem. 85 (1981) 2766–2771.
[5] E. Fernandez, J.M. Figuera, A. Tobar, Use of the potassium ferrioxalate actinometer below 254 nm, J. Photochem. 11 (1979) 69–71.
[6] R.O. Rahn, Use of potassium-iodide as a chemical actinometer, Photochem. Photobiol. 58 (1993) 874–880.
[7] R.O. Rahn, Potassium iodide as a chemical actinometer for 254 nm radiation: use of iodate as an electron scavenger, Photochem. Photobiol. 66 (1997) 450–455.
[8] R.O. Rahn, M.I. Stefany, J.R. Bolton, E. Goren, P.-S. Shaw, K.R. Lykke, Quantum yield of the iodide–iodate chemical actinometer: dependence on wavelength and concentration, Photochem. Photobiol. 78 (2003) 146–152.
[9] H.J. Kuhn, S.E. Braslavsky, R. Schmidt, Chemical actinometry, Pure Appl. Chem. 76 (2004) 2105–2146.
[10] S.L. Murov, Handbook of Photochemistry, Marcel Dekker Inc., 1993.
[11] D.E. Nicodem, O.M.V. Aquilera, Standartization of the potassium ferrioxalate actinometer over the temperature range 5–80 °C, J. Photochem. 22 (1983) 189–193.
[12] Q.G. Mulazzani, M. D'Angelantonio, M. Venturi, M.Z. Hoffmann, M.A. Rodgers, Interaction of formate and oxalate ions with radiation-generated radicals in aqueous solution. Methylviologen as a mechanistic probe, J. Phys. Chem. 90 (1986) 5347–5352.
[13] K.A. Hislop, J.R. Bolton, The photochemical generation of OH radicals in the UV–vis/ferrioxalate/H_2O_2 system, Environ. Sci. Technol. 33 (1999) 3119–3126.
[14] M.E. Balmer, B. Sulzberger, Atrazine degradation in irradiated iron/oxalate system: effects of pH and oxalate, Environ. Sci. Technol. 33 (1999) 2418–2424.